CrystEngComm

Accepted Manuscript

ROYAL SOCIETY OF CHEMISTRY

www.rsc.org/crystengcomm

Journal Name

ARTICLE

Proposal for Crystallization of 3-Amino-4-halo-5-methylisoxazoles: An Energetic and Topological Approach

Received 00th January 20xx,
Accepted 00th January 20xx

DOI: 10.1039/x0xx00000x

www.rsc.org/

M. A. P. Martins,[a†] A. R. Meyer,[a] A. Z. Tier,[a] K. Longhi,[b] L. C. Ducati,[c] H. G. Bonacorso,[a] N. Zanatta,[a] and C. P. Frizzo[a]

The supramolecular structure of 3-amino-4-halo-5-methylisoxazoles (with halo = Cl, Br, I) was investigated in order to suggest a route for crystallization of small molecules. The hierarchy of intermolecular interactions during the growth of the crystal was established by x-ray diffraction, ^{1}H NMR titration, QTAIM analysis and quantum mechanical calculations. The relationship between QTAIM and energetic data was the fundamental innovation in this work. It allowed the partitioning of the dimer interaction energy between interacting atoms. Partitioning shows the cooperation of intermolecular interactions in the stabilization of dimers and led to observation of the energetic consequences that small changes in the molecular structure of each compound may have on the crystal packing. The proposed route for crystallization of the supramolecular cluster was based on the energetic hierarchy, in which the hydrogen bond is the strongest interaction and the first to form, and the π-interactions are weaker than the hydrogen bond and cannot compete with it. However, the π-interactions are responsible for the growth of the crystal connecting the rising layers of the hydrogen bond dimers. The other interaction formed, the halogen bond, is too weak to compete with the other two interactions, but it is fundamental for linking the layer that leads to the final three-dimensional arrangement. Finally, a new way of understanding the crystallization process and the design of new materials is presented.

Introduction

How molecules aggregate in solution to form a crystal and what the relationship is between the molecular structure and the crystal structure are some of the big questions in crystal engineering.[1] Great insights into these questions can be obtained by deciphering the nucleation mechanism and the crystal growing process. Much effort has been devoted to increasing knowledge, and a wide range of techniques have been used in order to generate insights into the crystallization mechanism;[2-4] however, there still remain doubts about this process.

According to the Aufbau building-up process,[5] crystallization can be viewed in a stepwise manner, in which association of the molecules increases the complexity and leads to the crystal (one → few → many → nucleus → crystal). However, this process does not necessarily need to be continuous; for example, a midsize cluster may be formed but it is unable to grow further, which results in dissolution, and so an alternative pathway with growth possibilities needs to be found.[1] This emphasizes that the final crystal structure is not determinate only during the nucleation, and that the crystal growth rates of polymorphs play an important role in the final product of the crystallization process.[2]

Spectroscopy techniques give valuable information about the self-assembly of the molecules in the first steps of the crystallization;[3] for example, the concentration-dependent NMR spectroscopy that simulates these first steps in solution, in which the solvent slowly evaporates and the solution becomes saturated. With the increases in concentration, chemical shift changes occur. These changes show which parts of the molecule are involved in intermolecular interactions. From these data it can be suggested which molecular dimers will be the first formed. Computational approaches are also employed to generate insights at the molecular level of the nucleation.[6]

In previous works, our study group analyzed the crystal packing of a series of heterocyclic compounds, based on data obtained from single-crystal x-ray diffraction data.[7-10] Recently, we suggested a new approach for analyzing the arrangement in organic crystals.[11] This approach is a powerful tool because it analyzes all the interactions that form the crystal, which is the final product of the crystallization process.[11-13]

Our objective herein is to further our study of the analysis of the crystal packing of heterocycles, taking into account consequences arising from small changes in molecular

[a] Núcleo de Química de Heterociclos (NUQUIMHE), Departamento de Química, Centro de Ciências Naturais e Exatas, Universidade Federal de Santa Maria, 97.105-900, Santa Maria, RS, Brasil.
[b] Instituto Federal de Educação, Ciência e Tecnologia Farroupilha, CEP 98130-000, Júlio de Castilhos, RS, Brasil.
[c] Instituto de Química, Universidade de São Paulo, P.O. Box 26077, 05508-900 São Paulo, Brazil.
† mmartins@base.ufsm.br (Marcos A. P. Martins).
Electronic Supplementary Information (ESI) available: [details of any supplementary information available should be included here]. See DOI: 10.1039/x0xx00000x

structures, in order to suggest a possible route for crystallization and its final result in the crystal. For this purpose, ^{1}H NMR will be used to generate data for the first crystallization steps, and x-rays will be used to characterize the crystal packing and quantum mechanical calculations, in order to provide energetic data about the supramolecular interactions. Also, recourse to existing knowledge about nucleation and crystal growth will be taken into account. Three structures of 3-amino-4-halo-5-methylisoxazoles were selected, in which the only difference is the halogen atom attached at the 4 position of the isoxazole. These compounds are good models due to them having several functionalities present in their molecular structure which are of great interest in the crystal engineering field; for example: the amine group (hydrogen bond (HB) donor and acceptor); halogens (halogen bond (XB) donor or acceptor); and N and O (both XB and HB acceptors). Also, the isoxazole ring is a π-electron system (X···π-, C-H···π- or π···π-interactions) — **Figure 1**. Thus, this system can be useful in answering the following questions: which interactions are the most important for the growth of the crystal? And, what is the real importance of halogen bonds (XB) in a system containing hydrogen bonds (HB) and π···π-interactions?

Results and Discussion

The study of the crystallization of 3-amino-4-halo-5methylisoxazoles presented in this work is based primarily on the crystal packing of **1–3** from x-ray diffraction. The supramolecular cluster approach was used for the full characterization of all intermolecular interactions present in the crystals. The crystal growing in solution was evaluated by NMR analyses. Finally, results were connected in order to suggest a possible crystallization method. The molecular structures of compounds **1–3** are shown in **Figure 2**.

Topological and energetic aspects of the crystals of **1-3** were obtained from the supramolecular cluster approach.[11] The supramolecular cluster of a crystal is formed by a given central molecule (M1) that is in contact with other (MN) molecules and forms the first molecular coordination sphere.

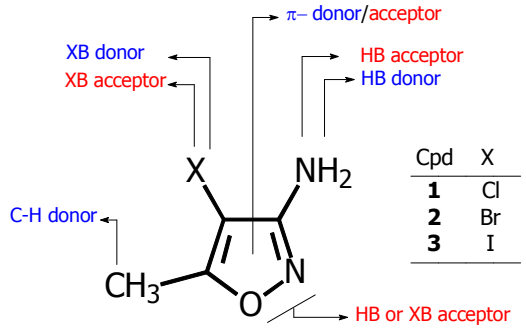

Figure 1. Functionalities present in the isoxazoles **1-3** which are of great interest in the crystal engineering field.

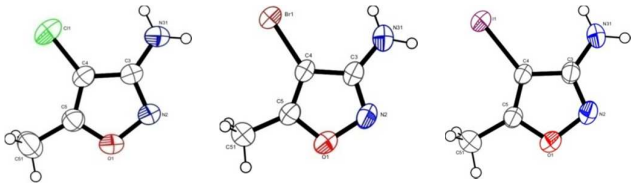

1 **2** **3**

Figure 2. Molecular structure of **1**, **2**, and **3** represented by ORTEP® diagram, with thermal ellipsoids drawn at the 50 % probability level.

The supramolecular cluster is considered to be the smallest portion of the crystal that contains the necessary information to understand the intermolecular interactions of the entire crystal. The supramolecular cluster of compounds **1–3** were determined and the molecular coordination number (MCN)[14-16] was found to be 14. In other words, the supramolecular cluster has one central molecule (M1) and 14 neighboring molecules (MN) in the first molecular coordination sphere. The interaction energy between the central molecule and each of its neighboring molecules (dimers $G_{M1\cdots MN}$) can be obtained by quantum mechanical calculations. The dimer interaction energies ($G_{M1\cdots MN}$) of **1–3** were obtained by the difference in energy between a dimer and the double monomer energy[11] at the MP2/cc-pVTZ level of theory. The sum of the interaction energies of all the dimers of a supramolecular cluster can be used as the estimation of the stabilization energy of the crystal ($G_{Cluster}$).[11] The dimer interaction energies and $G_{Cluster}$ for **1–3** are shown in **Table 1**.

Higher interaction energies were found in dimers M1···M2 and M1···M15, corresponding to 23–27 % and 15–19 % of cluster energy, respectively. The sum of the energy of dimers M1···M2 and M1···M15 corresponds to about 40 % of the cluster energy

Table 1. Interaction energies[a] of the dimers present in the clusters of compounds **1**-**3**.

Dimer	$G_{M1\cdots MN}$(kcal mol^{-1})		
	1	**2**	**3**
M1···M2	-8.33	-8.50	-8.73
M1···M3	-2.63	-1.53	-2.27
M1···M4	-0.37	-0.81	-0.72
M1···M5	-1.66	-1.30	-1.35
M1···M6	-0.37	-1.51	-2.25
M1···M7	-2.63	-1.80	-1.40
M1···M8	-0.69	-1.44	-1.22
M1···M9	-0.69	-1.43	-1.19
M1···M10	-1.66	-2.20	-2.21
M1···M11	-0.60	-2.20	-2.21
M1···M12	-0.60	-0.42	-0.82
M1···M13	-2.75	-0.87	-1.26
M1···M14	-2.75	-5.69	-6.29
M1···M15	-5.87	-5.25	-5.81
$G_{Cluster}$	-31.61	-34.94	-37.71

[a] Calculated at the MP2/cc-pVTZ level of theory.

which demonstrates the great contribution of these two dimers to the stabilization and growth of the crystal packing of compounds **1–3**. The energy contribution of the other dimers is lower and varies between compounds. Thus, in order to understand which structural and electronic properties of each molecule are affecting the dimer energy, a topological analysis of the dimers of supramolecular clusters was performed, based on the Quantum Theory of Atoms in Molecules (QTAIM). Topological analysis based on QTAIM is a powerful tool in the study of intermolecular interactions. The presence of the intermolecular interaction is given by a bond critical point (BCP) along the bond path connecting two interacting atoms.[17,18] All dimers of the supramolecular cluster of compounds **1–3** were submitted to QTAIM analysis, and the results are shown in **Table 2**. All dimers showed bond paths, thus confirming that 14 molecules of the first coordination sphere are interacting with the central molecule rising in the supramolecular clusters of compounds **1–3**. The QTAIM analysis (**Table 2**) showed that most of the dimers are interacting via more than one BCP (electronic density). Additionally, results showed that 60 to 90 % of cluster energy comes from dimers that have two and three BCP (electronic density) between dimer molecules. Dimers are showed with one BCP giving the atom···atom C-Br···O (**Figure 3a**); with two BCP giving the atom···atom N-H···N (**Figure 3b**); with three BCP giving one C-I···N and two N-H···H-N interactions (**Figure 3c**). Examples of dimers with four BCP, in which two BCP form a C-H···π interaction and the other two form a C-Cl···Cl and C-Cl···NH interaction are shown in **Figure 4a**. Two BCP forming a π···π interaction and two BCP forming two C-H···NH interactions are shown in **Figure 4b**. Finally, **Figure 4c** shows a dimer with five BCP, in which one BCP gives one π···π, two BCP give two C-Br···π interactions, and the other two BCP give two C-H···NH interactions. Several works have shown that the energy of an atom···atom interaction can be estimated from the electron density at the BCP.[17] In order to confirm this hypothesis for compounds **1–3**, the sum of electron density ($\Sigma\rho_{INT}$) at the BCP and the sum of the dimer energy was plotted. A good correlation (r = 0.931) was observed and the hypothesis aforementioned was confirmed for compounds **1–3** (See **Figure S1** in SI).

Because the energy contribution of atom···atom interactions for the stabilization for each dimer is proportional to ρ_{INT}, the energy contribution of atom···atom interactions can be estimated. The partitioning of the dimer interaction energy ($G_{M1\cdots Mn}$) into atom···atom interactions is proposed, in order to determine the energy contribution of each participant atom in the intermolecular interactions. The energy of each atom¨¨atom interaction ($G_{AI(X\cdots y)}$, where X = CH, NH, C-Halogen, π and Y = N, O, Halogen, HC, HN, π) was mathematically defined using **Eq. 1** and the ρ_{INT} at the BCP. The type of atom¨¨atom interactions and the ρ_{INT} used in the determination of G_{AI} for the atom¨¨atom interaction of compounds **1–3** are listed in **Table 2**.

$$G_{AI(X\cdots Y)} = \frac{G_{M1\cdots Mn}\cdot\rho_{INT}}{\Sigma\rho_{INT}} \qquad \text{Eq. 1}$$

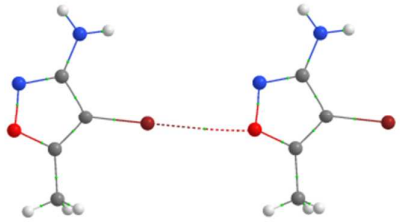

(a) (M3···M1, **2**)

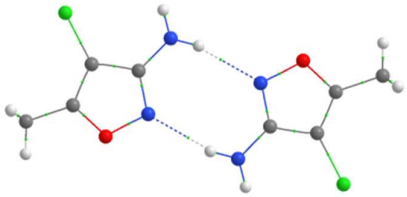

(b) (M1···M2, **1**)

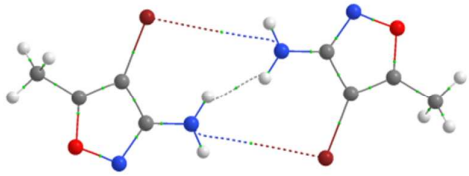

(c) (M1···M7, **2**)

Figure 3. View of the dimer interactions with: (a) one, (b) two, and (c) three BCP connecting interacting atoms.

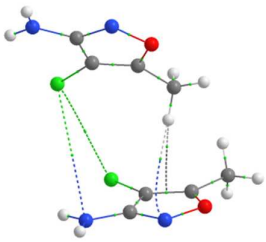

(a) M1···M13, **1**

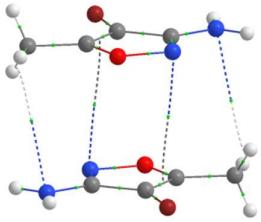

(b) M1···M14, **2**

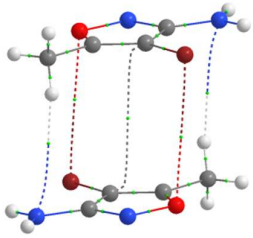

(c) M1···M15, **2**

Figure 4. View of the dimer interactions with: (a) four; (b) four; and (c) five bond paths connecting two interacting atoms.

Results of the partitioning of the dimer interaction energy show that dimer M1···M2, M1···M10, and M1···M12 of compounds **1–3** had the same interactions. For the other ten dimers, similar interactions were observed for compounds **2** and **3**, while very different interactions occurred for **1** (**Figure 5**). Partitioning the dimer interaction energy also shows the cooperation of intermolecular interactions in the stabilization of dimers. Dimer M1···M2 had only one strong (high energy) interaction. Most of other dimers have more than one interaction with low stabilization energy. Partitioning the dimer interaction energy using ρ_{INT} shows that binding energy determined for a pair of molecules (dimer) reflects the energy of all intermolecular interactions between two molecules and

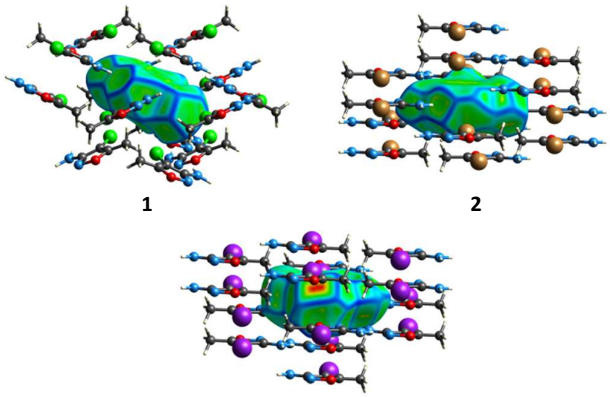

Figure 5. Hirshfeld Surface of M1 and supramolecular cluster for compounds **1**-**3**. Differences and similarities in the crystal packing of the compounds can be seen.

of one specific atom···atom interaction.This fact explains the high energy values found for the halogen bonds C-H···O(N), C-H···π, and π···π (2-8 kcal·mol^{-1}) in some crystal dimers described in the literature.[19-22] On the contrary, by partitioning the dimer interaction energy in specific atom···atom interactions, it is possible to estimate a reasonable value for the energies of intermolecular atom···atom interactions. The energy of each intermolecular interaction present in each dimer of compounds **1–3** was determined, and is expressed as G_{AI} in **Table 2**. An interesting observation about the energetic properties of each intermolecular interaction was revealed. It can be seen that the N-H···N is the most energetic interaction and it is the only interaction in dimer M1···M2 for compounds **1–3**. The stabilization energy of the dimer is given by two N-H···N, with stabilization energy of about -4.00 kcal·mol^{-1}. Geometric parameters of each interaction are given in SI. for compounds **1–3**, bond angle and distance was similar. The G_{AI} of the C-H···N interactions was similar for compounds **1–3** and the G_{AI} was about 1.15 kcal·mol^{-1}. An interesting observation is that the G_{AI} of C-H···X is similar for **1–3** and has a small angular dependence, while the G_{AI} of C-X···O increases from **1–3**, and geometric parameters depend on the halogen atom. For X = Cl (**1**), the G_{AI} decreases because of the angle (102°). The C-X···N interaction can be of two kinds: (i) invariable G_{AI} for **1–3** (average G_{AI} = -0.44) and an angle of 100°; and (ii) G_{AI} increases from **1** to **3**. The X···X interactions can also be of two kinds — G_{AI} increases from **1** to **3**, and the differences are related to halogen bond properties. The difference between the two kinds of interactions is in the geometric parameters. C-X···π interactions are only present in compounds **2** and **3**. These interactions have a small G_{AI} that increases from Cl to I. The C-H···π interaction is only present in **1** — the G_{AI} for two interactions is invariable. The difference between two interactions is in the superposition of rings that is given by angles that are 92–100° for one interaction and 126–127° for the other. Finally, H···H interactions were found to have G_{AI} in the range of -0.24 to -0.85. G_{AI} increases with the increase in distance between atoms. An important observation is that the G_{AI} of the N-H···HN interaction shows that the interaction is a simple H···H interaction and not a hydrogen bond[23].

Finally, a general observation takes into account the energy (G_{AI}) — greater differences in energy between compounds **1–3** are related to intermolecular interactions formed by halogen; for example, C-H···X, C-X···O, C-X···N, X···X, and X···π. Interestingly, these intermolecular interactions were the interactions responsible for the differences in the G_{AI} of compounds **1–3** (**Table 2**).

QTAIM analysis indicated that interactions involving iodine is greater than for chlorine, probably because the ρ_{INT} in the BCP is greater for iodine. The result can be confirmed by considering the molecular electrostatic potential (MEP). Based on the MEP, positive electrostatic surfaces are observed at the outer surface of covalently bonded halogens.[24] These regions are called σ-hole and can interact with negative sites in the same molecules or with others. The σ-hole increases from chorine to covalently bonded iodine.[25] Thus, QTAIM, MEP and energetic combined analysis showed the energetic dependency in relation to the halogen bond. The MEP were determined for compounds **1–3** in order to demonstrate that the σ-hole increases for compounds **1**, **2**, and **3**, which correspond to chlorine, bromine, and iodine σ-hole, respectively (**Figure 6**).

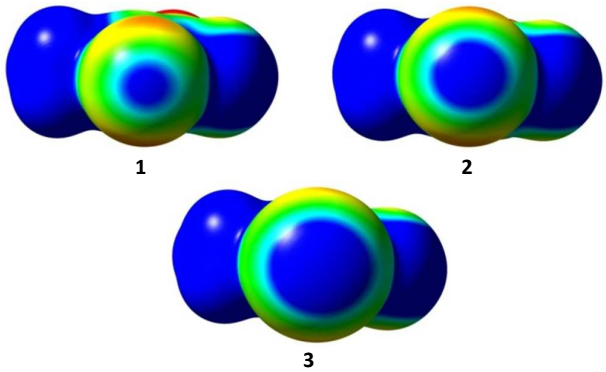

Figure 6. Molecular electrostatic potential: (a) upper view of ring; and (b) front view of halogen σ-hole (in blue) for compounds **1**, **2**, and **3** calculated with an isodensity value of

0.001 (red, -0.001 a.u.; yellow, -0.005 a.u.; green, 0.000 a.u.; and blue, +0.001 a.u.).

Table 2. The ρ_{INT} (from QTAIM)[a] and atom interaction energy (G_{AI})[b] for all dimers of compounds **1–3**.

	Atoms	**1**		Atoms	**2**		Atoms	**3**	
Dimer	Interaction	$\rho_{INT\ (u.a.)}$	$G_{AI(x\cdots Y)}$[b]	Interaction	$\rho_{INT\ (u.a.)}$	$G_{AI(x\cdots Y)}$[b]	Interaction	$\rho_{INT\ (u.a.)}$	$G_{AI(x\cdots Y)}$[b]
M1···M2	N···HN	0.015326	-4.17	N···HN	0.014235	-4.25	N···HN	0.014716	-4.36
	NH···N	0.015326	-4.17	NH···N	0.014235	-4.25	NH···N	0.014717	-4.37
M1···M3	O···HN	0.008197	-1.66	CBr···O	0.001118	-1.53	CI···O	0.008488	-2.27
	O···ClC	0.002279	-0.46						
	N···ClC	0.002483	-0.50						
M1···M4	CH···ClC	0.006021	-0.37	CH···HC	0.002393	-0.81	CH···HC	0.002189	-0.72
M1···M5	CCl···NH	0.001028	-0.42	CH···BrC	0.002415	-0.49	CH···IC	0.002925	-0.56
	CH···N	0.002989	-1.24	CH···HC	0.001549	-0.32	CH···HC	0.001234	-0.24
				CH···BrC	0.002415	-0.49	CH···IC	0.002925	-0.56
M1···M6	CH···ClC	0.006020	-0.37	CBr···O	0.005928	-1.51	CI···O	0.008487	-2.25
M1···M7	O···H-N	0.008197	-1.66	N···BrC	0.003856	-0.47	N···IC	0.004541	-0.43
	O···ClC	0.002279	-0.46	NH···HN	0.006959	-0.85	NH···HN	0.005562	-0.53
	N···ClC	0.002483	-0.50	N···BrC	0.003856	-0.47	N···IC	0.004541	-0.43
M1···M8	CH···ClC	0.002202	-0.69	CH···BrC	0.003938	-1.12	CH···IC	0.002930	-1.22
				NH···O	0.001118	-0.32			
M1···M9	CH···ClC	0.002203	-0.69	CH···BrC	0.003938	-1.11	CH···IC	0.002930	-1.19
				NH···O	0.001119	-0.32			
M1···M10	CH···N	0.002989	-1.24	CH···N	0.005617	-1.41	CH···N	0.004995	-1.23
	CCl···NH	0.001028	-0.42	CBr···NH	0.003177	-0.79	CI···NH	0.003976	-0.98
M1···M11	CCl···NH	0.002518	-0.60	CH···N	0.005617	-1.41	CH···N	0.004995	-1.23
				CBr···NH	0.003177	-0.79	CI···NH	0.003976	-0.98
M1···M12	CCl···N	0.002518	-0.60	CBr···BrC	0.000982	-0.42	CI···IC	0.002614	-0.82
M1···M13	CH···π	0.005263	-1.96	CBr···BrC	0.004107	-0.87	CI···IC	0.005753	-1.26
	CH···π	0.004368							
	CCl···ClC	0.001739	-0.35						
	CCl···NH	0.002123	-0.43						
M1···M14	CH···π	0.005263	-1.96	CH···N	0.002839	-1.03	CH···N	0.003291	-1.27
	CH···π	0.004368		π···π	0.005018	-3.64	π···π	0.004861	-3.76
	CCl···ClC	0.001739	-0.35		0.005018			0.004861	
	CCl···NH	0.002123	-0.43	CH···N	0.002839	-1.03	CH···N	0.003292	-1.27
M1···M15	CH···N	0.003899	-1.02	CH···N	0.003340	-1.01	CH···N	0.002898	-0.95
		0.003618		CBr···π	0.003474	-1.05	CI···π	0.004347	-1.42
	π···π	0.003681	-3.82	π···π	0.003773	-1.14	π···π	0.003293	-1.08
		0.003681		π···BrC	0.003474	-1.05	π··· IC	0.004347	-1.42
		0.003618		CH···N	0.003341	-1.01	CH···N	0.002899	-0.95
	N···HC	0.003899	-1.02						

[a]Quantum Theory of Atoms in Molecules; [b]Atom interaction energy ($G_{AI(X\cdots Y)}$) in kcal·mol^{-1}, where X = CH, NH, C-Halogen, π and Y = N, O, Halogen, HC, HN, π.

^{1}H NMR analyses

After the full characterization of the interactions present in the crystals of the isoxazoles, the next step was the investigation of the prenucleation of compounds **1–3** in solution. This study was performed using ^{1}H NMR solution in accordance with previous work published by Spitaleri et al.[3,26] These authors showed that it is possible to determine the first stage of the crystal nucleation process using ^{1}H NMR spectroscopy in solution. Dimers were detected by dilution of compounds and observation of the dependence of some signal's chemical shift on concentration. In accordance with Spitaleri et al.,[3,26] the dimer structures detected in solution are maintained throughout the additional stages of aggregation and crystal growth, and therefore they are found intact in the final crystal. The ^{1}H NMR dilution curves were constructed for compounds **1–3**. The dependence of the chemical shift on the concentration of the amino and methyl groups was evaluated in $CDCl_3$ and CD_3OD. In $CDCl_3$, the signal due to 3-NH_2 hydrogen shows a large (**Figure 7**) downfield change in chemical shift as the concentration increases, indicating the formation of a hydrogen bond. The signal due to 5-CH_3 hydrogen was an upfield shift due to the increase in concentration. The upfield shift is probably a result of the anisotropic effect due to the aromatic ring proximity. The strong interactions are given by association constants; for example, K_{ass} = 10.4 M^{-1} for N-H···N (NH_2). The association constant for π-interactions (C-H···π) was

lower (K_{ass} ~ 0.8 M^{-1}), which indicates that this interaction is performed in CD_3OD. The pattern of chemical shift change of signals due to the 5-CH_3 group was similar to that observed in $CDCl_3$ (K_{ass} ~ 0.7 M^{-1}). However, the chemical shift changes of the signal due to 3-NH_2 were neglected (K_{ass} ~ 0.0 M^{-1}) — see **Figure 8**. These results were expected and indicate the tendency towards a weak dimerization by N-H···N (NH_2) interaction in CD_3OD. Protic solvent competes with the dimer based in a self-assembling hydrogen bond, and the same solvent does not interfere with dimers based in π···π-probably weaker. The same titration experiment was interactions. These results are also in accordance with previous results described by Spitaleri et al.[3,26] for similar compounds, which showed that solvents have a great impact on the structure of the prenucleation aggregates. In addition, NMR experiments show that in 1M solution the dimer is the predominant form in the solution, and that the ^{1}H NMR maximum variation for association by N-H···N (NH_2) interaction in $CDCl_3$ was 1.55 ppm.

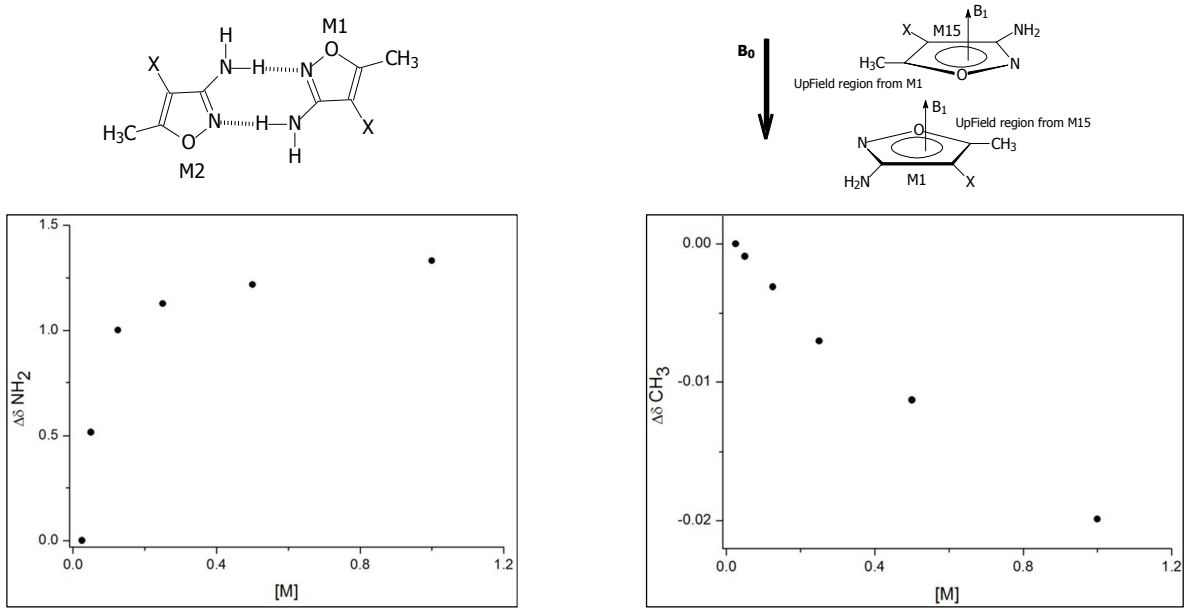

Figure 7.^{1}H NMR chemical shift changes of signals due to 3-NH_2 and 5-CH_3 **2** in $CDCl_3$.

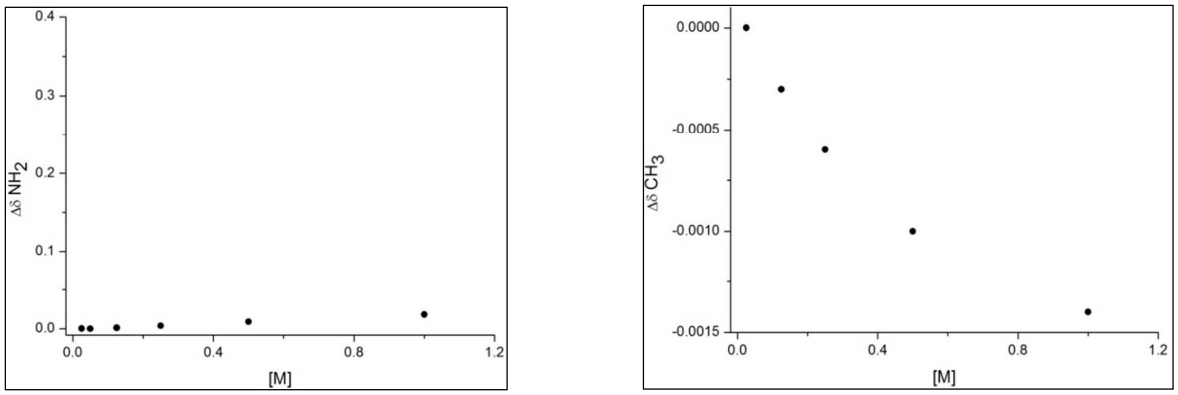

Figure 8.^{1}H NMR chemical shift changes of signals due to 3-NH_2 and 5-CH_3 **2** in CD_3OD.

These observations are also consistent with the aforementioned result from QTAIM and dimer energy, which show that there are the two strongest N-H···N hydrogen bonds in dimer M1···M2 for compounds **1–3**. In addition, π-interactions are the second strongest interaction and are responsible for the formation of dimer M1···M15 (**Figure 7**).

Proposed crystallization mechanism

After analyzing the crystal packing of isoxazoles and evaluating the first steps of crystallization in solution, we were able to propose a crystal growing model for **1–3**.

Compound **1** crystallizes in the orthorhombic crystal system, while compounds **2** and **3** crystallize in the monoclinic system. The difference between the crystal packing of **1** and that of **2**

and **3** can also be viewed in the supramolecular clusters (**Figure 3**). In terms of intermolecular interactions, these changes are related to the π···π-interactions (present in **2** and **3**) which are replaced by CH-π-interactions in **1** (see dimers M1···M13, M1···14, M1···15 in **Table 2**). These differences in the crystal packing of compounds **1**, **2**, and **3** are intriguing because their molecular structure differs only in the halogen atom attached at the 4-position of the ring. Taking into account the molecular structure of **1–3**, and based on the observations of dimers and supramolecular cluster energy, NMR and x-ray diffraction analysis, some insights about these differences are described in order to suggest the crystallization method for **1–3**. According to the theory of the hierarchy of intermolecular interactions,[27,28] during the crystallization process the formation of the strongest interactions occurs first, and then the formation of weaker interactions occurs at the remaining sites. Considering compounds **2** and **3**, the most energetic dimer was M1···M2, which is stabilized by two N-H···N hydrogen bonds (see **Figure 3b**). This interaction links two molecules, thus forming the dimer with average energy of -8.5 kcal mol^{-1} (Stage I, **Figure 9**). The second strongest dimer was the M1···M14 (for compounds **2** and **3**), which is the dimer formed by π···π- and other interactions, and whose total energy was about -6.0 kcal mol^{-1}. These π-interactions link the dimers formed by N-H···N hydrogen bonds and form infinite chains along the *ab* direction (Stage II, **Figure 9**). Following the dimer energy hierarchy, the next strongest dimer is the M1···M15 with -5.6 kcal mol^{-1}, which forms a π-interaction that connects the one-dimensional infinite chains (also formed by the π-interaction), resulting in a two-dimensional layer in the *ac* direction (Stage III, **Figure 9**). After the layer formation, only the halogen atom remains as a site for intermolecular interactions. In these sites the formation of the interaction that will link the layers forming the three-dimensional crystal occurs. The layers are connected by C-X···O interactions, and this connection is intensified by weak interactions between the amine groups (Stage IV, **Figure 9**). In summary, in **2** and **3**, the monomers are connected by N-H···N hydrogen bonds forming dimers. These dimers are connected by π-interactions which form one-dimensional infinite chains. These chains are linked by π-interaction which results in two-dimensional chains, and then the chains are connected by C-X···O halogen bonds to form the three-dimensional crystal (**Figure 9**). In the same manner, we can analyze crystal growing**.** Bearing in mind dimer energies, similarities in the clusters of **1–3** were investigated and points where changes occur were revealed. Similar to compounds **2** and **3**, the first two stages of the crystallization of compound **1** were the formation of dimer M1···M2 (N-H···N interaction with -8.33 kcal mol^{-1}) followed by dimer M1···M15 (π-interaction and other interactions stabilized by -5.87 kcal mol^{-1}), which connect the dimers formed by the hydrogen bonds and form one-dimensional infinite chains (Stage II). Changes in the crystal growing of **1** started after this point. Instead of the formation of the second π-interaction to the connected one-dimensional infinite chains, a C-H···π interaction was observed, which formed M1···M13 and M1···M14 dimers with stabilization energy of -2.75 kcal mol^{-1} for each one. These two C-H···π interactions have a cooperative effect, in which M1 is involved with two other molecules (M13 and M14). This cooperation results in a total energy of -5.50 kcal mol^{-1}, which is similar to the energy of the π-interaction forming a two-dimensional layer in **2** and **3**. The C-H···π interactions in **1** link the one-dimensional infinite chain formed, thereby yielding two-dimensional layers (Stage III). After the layer formation, the remaining interaction sites are the same as in the other two compounds — chlorine atom in this case. One interesting point is that compound **1** does not show how the C-Cl···O halogen bonding occurs in the crystal packing of **2** and **3**. On the contrary, the oxygen atom of the ring interacts with the available N-H of the amine group, forming an N-H···O interaction with energy of -1.66 kcal mol^{-1} in the dimers M1···M5 and M1···M10.

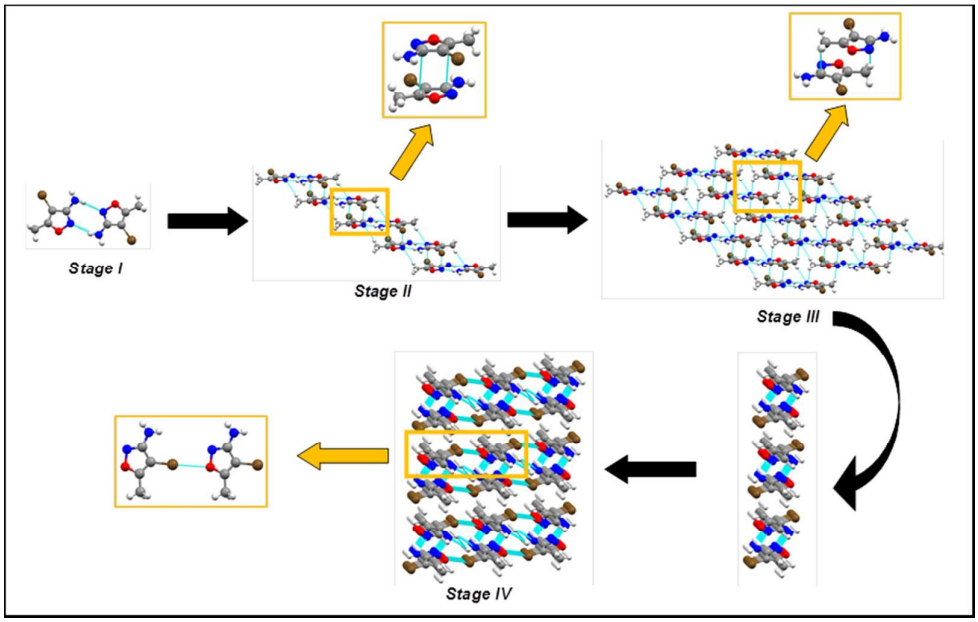

Figure 9. Possible growth route for the crystal of **2** (similar for compound **3**). Performed by Mercury® 3.1 software.[29]

This interaction is intensified by two other weak interactions of -2.63 kcal mol^{-1} (dimer M1···M7). These N-H···O interactions connect the layers, which results in the three-dimensional crystal (Stage IV). In summary, in the crystal packing of **1**, first the monomers are connected by N-H···N hydrogen bonds to form dimers. Subsequently, these dimers are connected by π-interactions, which leads to one-dimensional infinite chains. These chains are linked by C-H···π interactions (and other minor interactions) to form layers, and, finally, these layers are connected by N-H···O hydrogen bonds in the entire crystal (**Figure 10**).

Experimental fusion enthalpy was collected for compounds **1**–**3** and follows the same trend as that observed for the determination of $G_{cluster}$. The stablest crystal was from compound **3**, followed by compound **2**, and finally compound **1**. The crystalline packing efficiency (CPE)[13] of compounds **1**–**3** was determined. The CPE represents an estimation of molecules that are occupying the unity cell, as well as giving an idea of how close the molecules are in the unity cell — the closer they are, the more efficient the packing. For less polar compounds, it was observed that more efficient crystal packing results in greater energy stabilization. However, there are too few compounds to establish a correlation, and the CPE does not show a tendency. The CPE of compound **1** was less than for compounds **2** and **3**, which have the same CPE. The experimental fusion enthalpy, $G_{Cluster}$, and CPE of **1**–**3** are given in **Table 3**.

Table 3. Experimental fusion enthalpy, $G_{Cluster}$, and CPE of **1**–**3**.

	ΔH_m (kcalmol^{-1})[a]	Crystal void[b]	Cell vol.[b]	$G_{Cluster}$ (kcalmol^{-1})	CPE[c]
1	3.53	181.8	1204.2	-31.61	0.85
2	4.17	24.2	299.9	-34.94	0.92
3	4.64	26.3	323.0	-37.71	0.92

[a]Determined from DSC. [b]Å^2, obtained with Crystal Explorer® 3.1 software.[30] [c]Crystal packing efficiency (CPE) = (Cell Volume - Crystal Void)/Cell Volume

Conclusion

In this paper, results concerning the synthesis, crystallization, theoretical calculation (energetic dimers and QTAIM analyses), and ^{1}H NMR titration of three model compounds are reported. A possible crystallization mechanism for the isoxazoles **1**–**3** was presented. This proposal was based on the observation of the energetic consequences that small changes in the molecular structure of each compound may have on the crystal packing.

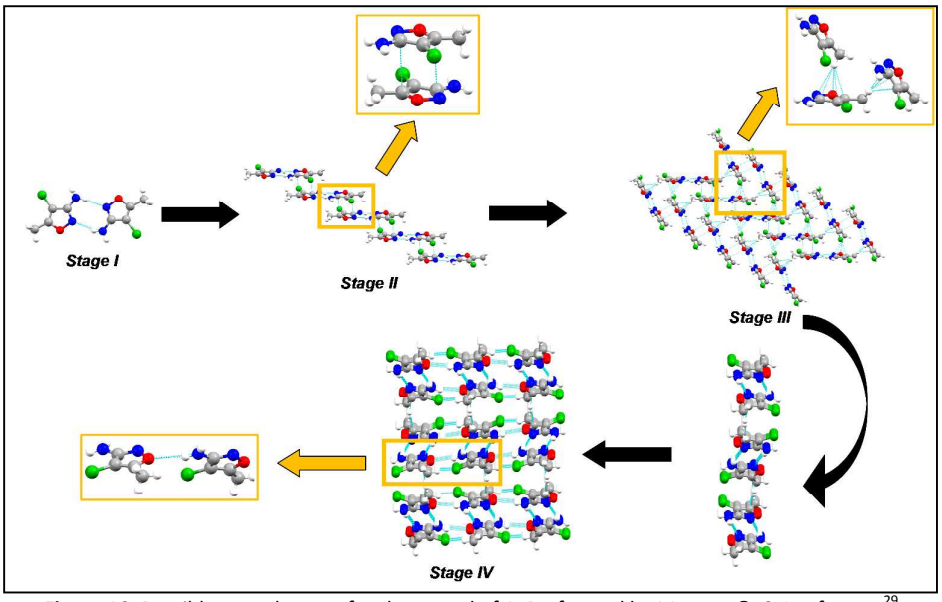

Figure 10. Possible growth route for the crystal of **1.** Performed by Mercury® 3.1 software.[29]

These changes arise due to the wide variety of intermolecular interactions, including hydrogen bonds, halogen bonds, and π-interactions, that are involved in the crystal packing of 1–3. The interactions analyzed here connect the several molecules that make up the first coordination sphere of isoxazoles 1–3. The results presented show that the supramolecular cluster has a energetic hierarchy related to the formation of interactions, in which the hydrogen bond is the strongest interaction and the first to form, and the π-interactions are weaker than the hydrogen bond and cannot compete with it. However, the π-interactions are responsible for the growth of the crystal connecting the rising layers of the hydrogen bond dimers. The other interaction formed, the halogen bond, is too weak to compete with the other two interactions, but it is fundamental for linking the layer that leads to the final three-dimensional arrangement. In proposing a growth route for the crystal, we verified the involvement of various stages of molecular aggregation. This process is similar for compounds 2 and 3, but different for compound 1 (due to system sensitivity in molecular changes). Finally, the present work offers a new way of understanding the crystallization process and the design of new materials based on 3-amino-4-halo-5-methylisoxazoles.

Experimental

Synthesis

The 3-amino-4-halo-5-methylisoxazoles **1–3** were synthesized by halogenation reaction of the 3-amino-5-methylisoxazole with *N*-chlorosuccinimide, *N*-bromosuccinimide, and *N*-iodosuccinimide, respectively. The aminoisoxazoles were dissolved in acetic acid and the *N*-halosuccinimide was slowly added in small aliquots over a period of 15 min, and then the reaction remained under magnetic stirring for 30 min at room temperature. The product was extracted with dichloromethane and aqueous solution of K_2CO_3 (0.5 M) and the organic phase was washed three times with distilled water. The organic phase was then dried with anhydrous sodium sulfate and the solvent was evaporated under reduced pressure. The product was purified by recrystallization from hexane. Single crystals of the products 3-amino-4-chloro-5-methylisoxazole (**1**), 3-amino-4-bromo-5-methylisoxazole (**2**), and 3-amino-4-iodo-5-methylisoxazole (**3**) were obtained by dissolving then (50 mg) in hexane (3 mL) and then slowly evaporating the resulting mixture at room temperature.

Single-crystal structure determination

The diffraction measurements were performed using graphite monochromatized Mo Kα radiation (k = 0.71073 Å), on a Bruker SMART APEXII CCD diffractometer.[31] The structures were solved with direct methods using the SHELXS program, and refined on F^2 by full-matrix least-squares with the SHELXL package.[32] The absorption correction was performed by the Gaussian method.[33] Anisotropic displacement parameters for non-hydrogen atoms were applied. The hydrogen atoms were placed at calculated positions with 0.96 Å (methyl CH_3), 0.93 Å (aromatic CH), and 0.82 Å (NH), using a riding model. Hydrogen isotropic thermal parameters were kept at $U_{iso}(H) = xU_{eq}$ (carrier C atom), with x = 1.5 for methyl groups and x = 1.2 for all other groups. The valence angles C–C–H and H–C–H of the methyl groups were set to 109.5°, and the H atoms were allowed to rotate around the C–C bond. Molecular graphs were prepared using ORTEP for Windows. Parameters in CIF format are available as an Electronic Supplementary Publication from the Cambridge Crystallographic Data Centre (CCDC 1405887 (**1**), 1405888 (**2**), 993666 (**3**)). Data collection and structure refinement for the structures of **1–3** are given in **Table 4**.

Table 4. Data collection and structure refinement for the structures of **1**–**3**.

Compound[a]	**1**	**2**	**3**
Empirical formula	$C_4H_5ClN_2O$	$C_4H_5BrN_2O$	$C_4H_5IN_2O$
Molecular weight	132.55	177.01	224.0
Temperature (K)	293(2)	293(2)	293(2)
Crystal system	Orthorhombic	Triclinic	Triclinic
Space group	Pbca	P-1	P-1
Cell parameters			
a (Å)	6.9082(3)	6.4176(7)	6.5261(3)
b (Å)	12.2055(7)	7.1023(9)	7.3488(3)
c (Å)	14.2820(8)	7.5370(10)	7.6401(3)
α (°)	90	94.502(8)	96.998(3)
β (°)	90	100.535(7)	100.396(3)
γ (°)	90	115.558(6)	113.411(3)
V (Å^3)	1204.23(11)	299.86(6)	323.04(2)
Z	8	2	2
Calcd. density (g.cm^{-3})	1.462	1.960	2.303
Abs. Coef. (mm^{-1})	0.531	6.750	4.861
F (000)	544	172	208
Crystal size (mm)	0.89 x 0.59 x 0.26	0.544 x 0.267 x 0.168	0.23 x 0.16 x 0.15
θ range for data collection (deg)	2.85 to 27.19	2.79 to 27.31	2.78 to 27.13
h,k,l range	$-8 \le h \le 8$ $-15 \le k \le 15$ $-18 \le l \le 18$	$-8 \le h \le 8$ $-9 \le k \le 9$ $-9 \le l \le 9$	$-8 \le h \le 8$ $-9 \le k \le 9$ $-9 \le l \le 9$
Reflections collected/unique	14204/ 1331 [R(int) = 0.0240]	7575/ 1349 [R(int) = 0.0279]	9332/ 1432 [R(int) = 0.0275]
Data/restraints/parameters	1331 / 0 / 73	1349 / 0/ 73	1432 / 0 / 73
Absorption correction	Gaussian	Gaussian	Gaussian
Refinement method	Full-matrix least-squares on (F^2)	Full-matrix least-squares on (F^2)	Full-matrix least-squares on (F^2)
Final *R* indices	R1=0.0467, wR2=0.1322	R1=0.0236, wR2=0.0575	R1=0.0219, wR2=0.0512
R all data	R1=0.0557, wR2=0.1455	R1=0.0331, wR2=0.0610	R1=0.0256, wR2=0.0531
Goodness of fit on F^2	1.058	1.051	1.074
Largest diff. peak and hole (e Å^{-3})	0.408 and -0.302	0.262 and -0.287	0.358 and -0.720

[a]Compound **3** data is already shown in Ref. 11.

Determination of MCN of supramolecular cluster

The supramolecular clusters were constructed based on the central molecule M1 and the MN (M2, M3, M4, …, MN) molecules surrounding it, which are present in its first coordination sphere. For this method we used the CrystalExplorer version 3.1[30] and TOPOS® version 4.0 softwares[34] andto determine all the molecules that are in contact with the M1 molecule. The cluster was fragmented into dimers based on the interaction of M1 with each of the MN molecules. For example, the M1···M2 dimer is the dimer formed between the molecules M1 and the M2.

Computational details

All theoretical calculations were done with the Gaussian® version 09, Revision A.1 package of programs.[35] Molecular geometries were taken from x-ray crystallographic data. Single point calculations were performed in order to obtain the intermolecular interaction energy between the molecular dimers. The Boys and Bernardi counterpoise method was employed in order to take into account the basis set superposition error (BSSE).[36] All quantum chemical calculations were performed at the MP2/cc-pVTZ level of theory. For the iodine atom, the cc-pVTZ-PP basis set was used to take into account the relativistic effects. Due to its accurate interaction energy description at a feasible computational cost, the second order Moller-Plesset perturbation theory (MP2) has been widely used for a long time to describe intermolecular interactions. However, this method has a high basis set dependency, and shows best results associated with the cc-pVTZ basis set.[37,38]

Quantum Theory of Atoms in Molecules (QTAIM) data All QTAIM analyses were performed with the aid of the AIMALL package of programs. The wavefunctions used in the QTAIM analyses were generated at the MP2/cc-pVTZ level of theory. The bond paths show which atoms are interacting and the

analyses of the electron density at the BCP provide important information about the intermolecular interactions. The electron density (ρ) value at the BCP is related to the intermolecular interaction strength — the greater the ρ value the greater the interaction energy. The Laplacian of the electron density ($\nabla^2\rho$) shows the nature of the interaction. Positive $\nabla^2\rho$ values indicate that the interaction is electrostatic in nature (ionic interactions, hydrogen bonds, halogen bonds), while negative Laplacian values indicate that the interaction is covalent in nature.[17,39]

Association constants obtained by ^{1}H NMR spectroscopy

^{1}H NMR dilution experiments were performed by preparing different dilutions of each compound at a known concentration; for example: compound **1** (1.8, 1.0, 0.5, 0.25, 0.125, 0.05, and 0.025 M); compound **2** (1.0, 0.5, 0.25, 0.125, 0.05, and 0.025 M); and compound **3** (1.5, 1.0, 0.5, 0.25, 0.125, 0.05, and 0.025 M). The ^{1}H NMR spectrum was recorded for each concentration. All the NMR spectra were recorded using a Bruker Avance III 600 MHz (^{1}H at 600.168 MHz). ^{1}H spectra were recorded in 5 mm sample tubes at 298 K (digital resolution of ± 0.01 ppm) in $CDCl_3$-d_6 or CD_3OD-d_6, using TMS as the internal reference.

Acknowledgements

The authors are grateful for the financial support from: the National Council for Scientific and Technological Development (CNPq) — Universal/Proc. 474895/2013-0 and Universal/ Proc. 475556/2012-7; the Rio Grande do Sul Foundation for Research Support (FAPERGS) — Proc. 2262-2551/14-1 and 2290-2551/14-1); and the Coordination for Improvement of Higher Education Personnel (CAPES/PROEX). The fellowships from CNPq (M.A.P.M, H.G.B., N.Z.) and CAPES (A.Z.T. and A.R.M.) are also acknowledged.

References

1 G. R. Desiraju, J. Am. Chem. Soc. 2013, 135, 9952 – 9967.
2 R. J. Davey, S. L. M. Schroeder and J. H. ter Horst, Angew. Chem. Int. Ed. 2013, 52, 2166 – 2179.
3 C. A. Hunter, J. F. McCabe and A. Spitaleri, CrystEngComm , 2012, 14 , 7115–7117.
4 S. A. Kulkarni, E. S. McGarrity, H. Meekesc and J. H. ter Horsta, Chem. Commun., 2012, 48, 4983–4985.
5 P. Ganguly and G. R. Desiraju, CrystEngComm, 2010, 12, 817–833.
6 J. Anwar and D. Zahn, Angew. Chem . Int. Ed. 2011, 50, 1996 – 2013.
7 C. P. Frizzo, E. Scapin, P. T. Campos, D. N. Moreira, M. A.P. Martins, Journal of Molecular Structure, 933, 142-147, 2009.
8 M. A. P. Martins, D. N. Moreira, C. P. Frizzo, P. T. Campos, K. Longhi, M. R.B. Marzari, N. Zanatta, H. G. Bonacorso, Journal of Molecular Structure, 969, 111-119, 2010.
9 C. P. Frizzo, A. R. Meyer, G. S. Caleffi, L. V. Rodrigues, M. R. B. Marzari, P. T. Campos, D. N. Moreira, H. G. Bonacorso, N. Zanatta, M. A. P. Martins, Journal of Molecular Structure, 1004, 45-50, 2011.
10 P. T. Campos, P. Machado, C. P. Frizzo, D. N. Moreira, A. R. Meyer, H. G. Bonacorso, N. Zanatta, L. C. Ducati, R. Rittner, C. F. Tormena, M. A. P. Martins, Journal of Molecular Structure (Print), 2011, 1006, 462-468.
11 M. A. P. Martins, C. P. Frizzo, A. C. L. Martins, A. Z. Tier, I. M. Gindri, A. R. Meyer, H. G. Bonacorso and N. Zanatta, RSC Adv., 2014, 4, 44337 – 44349.
12 C. P. Frizzo, C. R. Bender, A. Z. Tier, I. M. Gindri, P. R. S. Salbego, A. R. Meyer and M. A. P. Martins, CrystEngComm 2015, 17, 2996-3004,.
13 C. P. Frizzo, A. Z. Tier, I. M. Gindri, A. R. Meyer, G. Black, A. L. Belladona and M. A. P. Martins, CrystEngComm 2015, 17, 4325 – 4333.
14 A. I. Kitaigorodskii, Molecular Crystals and Molecules, Academic Press, New York, 1973.
15 W. Fischer and E. Koch, Z. Kristallogr., 1979, 150, 245–260.
16 T. G. Mitina and V. A. Blatov, Cryst. Growth Des. 2013, 13,1655–1664.
17 R. Bader Chem. Rev.; 1991, *91*, 893-928.
18 E. Arunan, G. R. Desiraju, R. A. Klein, J. Sadlej, S. Scheiner, I. Alkorta, D. C. Clary, R. H. Crabtree, J. J. Dannenberg, P. Hobza, H. G. Kjaergaard, A. C. Legon, B. Mennucci and D. J. Nesbitt, Pure Appl. Chem. 2011, 83, 1637-1641.
19 H. R. Khavasi, F. Norouzi and A. A. Tehrani, Crystal Growth & Design, 2015, 15, 2579-2583.
20 H. R. Khavasi and A. A. Tehrania, CrystEngComm, 2013,15, 3222-3235.
21 P. Panini, R. Shukla, T. P. Mohan, B. Vishalakshi and D. Chopra, J. Chem. Science, 126, 2014, 1337 - 1345.
22 D. Dey and D. Chopra J. Chem. Crystallogr. 2014, 44, 450-458.
23 D. Danovich, S. Shaik, F. Neese, J. Echeverría, G. Aullón and S. Alvarez J. Chem. Theory Comput. 2013, 9, 1977−1991.
24 P. Politzer, P. Lane, M. C. Concha, Y. Ma and J. S. Murray, J. Mol. Model 2007, 13, 305 - 311.
25 P. Politzer, J. S. Murray and T. Clarkcd, Phys. Chem. Chem. Phys. 2013, 15, 11178 - 11189.
26 A. Spitaleri, C. A. Hunter, J. F. McCabe, M. J. Packerc and S. L. Cockroft, CrystEngComm 2004, 6, 489-493
27 G. R. Desiraju, Angew. Chem. Int. Ed. 2007, 46 , 8342-8356
28 G. M. Espallargas, F. Zordan, L. A. Marín, H. Adams, K. Shankland, J. van de Streek and L. Brammer, Chem. Eur. J. 2009, 15, 7554 - 7568.
29 Mercury 3.1, The Cambridge Crystallographic Data Centre, 2012.
30 CrystalExplorer (Version 3.1), S.K. Wolff, D.J. Grimwood, J.J. McKinnon, M.J. Turner, D. Jayatilaka, M.A. Spackman, University of Western Australia, Perth, 2012.
31 Bruker, APEX2 (Version 2.1), COSMO (Version 1.56), BIS (Version 2.0.1.9) SAINT (Version 7.3A) and SADABS (Version 2004/1) and XPREP (Version 2005/4), Bruker AXS Inc., Madison, Wisconsin, USA, 2006.
32 G. M. Sheldrick, Acta Crystallogr., Sect. A: Found. Crystallogr., 2008, 64, 112–122.
33 P. Coppens, L. Leiserowitz and D. Rabinovich, Acta Crystallogr., 1965, 18, 1035–1038.
34 TOPOS version 4.0 software; V. A. Blatov and A. P. Shevchenko, Samara State University, Ac. Pavlov St., 443011 Samara, Russia, 2012.
35 Gaussian version 09, Revision A.1, M. J. Frisch, G. W. Trucks, H. B. Schlegel, G. E. Scuseria, M. A. Robb, J. R. Cheeseman, G. Scalmani, V. Barone, B. Mennucci, G. A. Petersson, H. Nakatsuji, M. Caricato, X. Li, H. P. Hratchian, A. F. Izmaylov, J. Bloino, G. Zheng, J. L. Sonnenberg, M. Hada, M. Ehara, K. Toyota, R. Fukuda, J. Hasegawa, M. Ishida, T. Nakajima, Y. Honda, O. Kitao, H. Nakai, T. Vreven, J. A. Montgomery, Jr., J. E. Peralta, F. Ogliaro, M. Bearpark, J. J. Heyd, E. Brothers, K. N. Kudin, V. N. Staroverov, R. Kobayashi, J. Normand, K. Raghavachari, A. Rendell, J. C. Burant, S. S. Iyengar, J. Tomasi, M. Cossi, N. Rega, J. M. Millam, M. Klene, J. E. Knox, J. B.

Cross, V. Bakken, C. Adamo, J. Jaramillo, R. Gomperts, R. E. Stratmann, O. Yazyev, A. J. Austin, R. Cammi, C. Pomelli, J. W. Ochterski, R. L. Martin, K. Morokuma, V. G. Zakrzewski, G. A. Voth, P. Salvador, J. J. Dannenberg, S. Dapprich, A. D. Daniels, Ö. Farkas, J. B. Foresman, J. V. Ortiz, J. Cioslowski and D. J. Fox, Gaussian, Inc., Wallingford CT, 2009.

36 S. F. Boys and F. Bernardi, Mol. Phys., 1970, 19, 553 - 566.

37 K. E. Riley and P. Hobza, J. Phys. Chem. A 2007, 111, 8257-8263.

38 K. E. Riley, J. A. Platts, J. Řezáč P. Hobza, and J. G. Hill, J. Phys. Chem. A 2012, 116, 4159 - 4169.

39 N. Han, Y. Zeng, C. Sun, X. Li, Z. Sun and L. Meng, J. Phys. Chem. A 2014, 118, 7058-7065

Graphical Abstract